EFFECTS OF GROWTH PARAMETERS ON THE SYNTHESIS AND CHARACTERISTICS OF APCVD GROWN GRAPHENE FOR PHOTOSENSING APPLICATIONS

RAED ABDELMAJEED MOHAMMAD ABDALRHEEM

UNIVERSITI SAINS MALAYSIA

2020

EFFECTS OF GROWTH PARAMETERS ON THE SYNTHESIS AND CHARACTERISTICS OF APCVD GROWN GRAPHENE FOR PHOTOSENSING APPLICATIONS

by

RAED ABDELMAJEED MOHAMMAD ABDALRHEEM

Thesis submitted in fulfilment of the requirements
for the degree of
Doctor of Philosophy

July 2020

ACKNOWLEDGEMENT

Praise and thanks to Allah first and foremost for his grace and virtue, who gave me life, health and ability to accomplish. I would also like to thank my main supervisor, Dr. YAM FONG KWONG, who honored me with his good manners and support for three years, and I would like to thank him for his scientific and useful comments that have significantly contributed to the accomplishment of this work. I was lucky that I was a student under the supervision of this great scientific stature. I would also like to thank my co-supervisors Prof. Dr. ABDUL RAZAK IBRAHIM and Dr. LIM HWEE SAN for their upscale dealings, cooperation, and support throughout this study. I would also like to thank my friend Dr. BEH KHI POAY for his valuable scientific comments and high-end ethics. I would also like to thank the NOR lab staff for their cooperation and assistance.

My heartfelt gratitude also goes to my family members: to my father, my wife and kids, brothers and sisters for their continuous prayers, and endless support when I needed it. Many thanks to all my friends and colleagues who supported and helped me at the School of Physics, University Sains Malaysia.

RAED ABDALRHEEM

2020

Penang, Malaysia

TABLE OF CONTENTS

LIST OF TABLES

Page

LIST OF FIGURES

Page

LIST OF ABBREVIATIONS

0D	Zero-dimensional
1D	One-dimensional
2D	Two-dimensional
3D	Three-dimensional
$FWHM_{2D}$	Full width at half maximum of 2D Raman peak
1L	One-layer
AFM	Atomic force microscopy
APCVD	Atmospheric pressure chemical vapor deposition
C.B	Conduction band
CME	Chemical metal etching
CRT	Cathode-ray tube
CVD	Chemical vapor deposition
CXR	Characteristic X-rays
DFT	Density functional theory
DMF	N, N-dimethylformamide
DVD	Digital versatile disc
ECD	Electrochemical delamination
EDX	Energy dispersive X-ray spectroscopy
EM	Electromagnetic
eV	Electron volte
FESEM	Field emission scanning electron microscopy
FETs	Field-effect transistors
FT-NMR	Fourier-Transform Nuclear Magnetic Resonance

GO	Graphene Oxide
Gr/p-Si	Graphene /p-type silicon
G pa	Giga pascal
HOPG	Highly oriented pyrolytic graphite
Hz	Hertz
IR	Infrared
iTA	In-plane transverse acoustic phonon
iTO	In-plane transverse optic phonon
LA	Longitudinal acoustic phonon
LEDs	Light emitting diodes
LO	Longitudinal optic phonon
LPCVD	Low pressure chemical vapor deposition
M	Molarity
MC	Monte Carlo
MD	Molecular dynamics
MFC	Mass Flow Controller
MP	Melting point
MSM	Metal-semiconductor-metal
Ni/Gr/n-Si	Nickel/graphene/n-type silicon
NIR	Near-infrared
n-type	Negative type
O-CGs	Oxygen-containing groups
OPA	1-octyl phosphonic acid
oTA	Out-of-plane transverse acoustic phonon
oTO	Out-of-plane transverse optic phonon

PAHs	Polyaromatic-aromatic-hydrocarbons
PDs	Photodetectors
PMMA	poly (methyl methacrylate)
p-type	Positive type
RF	Radio frequency
r-GO	Reduced graphene oxide
RS	Raman spectroscopy
RT	Room temperature
Sccm	Standard cubic centimeter per minute
SE	Secondary electrons
Sub-A	Sublattice A
TEC	Thermal expansion coefficient
TEM	Transmission electron microscopy
TRT	Thermal release tape
TVs	Televisions
UHV	Ultra-high vacuum
UV	Ultraviolet
V.B	Valance band
Vis	Visible
VS	Vapor-solid
XPS	X-ray Photoelectron Spectroscopy

LIST OF SYMBOLS

ϕ	Work function
ϕ_B	Barrier height
φ_s	Work function of spectrometer
ϕ_M	Metal work function
ϕ_p	Work function of p-type semiconductor
ϕ_n	Work function of n-type semiconductor
Φ_{Si}	Silicon work function
Φ_{Gr}	Graphene work function
χ_{Si}	Electron affinity of silicon
$\hbar$	Planck constant over 2 π
ξ	Fractional number of the absorbed photons
λ_o	Incident laser wavelength
λ_s	Scattered photon wavelength
Γ	Symmetry point at the center of Brillouin zone
ν	Frequency
ν_o	Incident photon frequency
ν_s	Scattered photon frequency
ν_m	Lattice frequency
v_F	Fermi velocity
Å	Angstrom ~ 10^{-10}m
A	Ampere
e	Charge of electron
B.E	Binding energy

E_g	Energy bandgap
E_F	Fermi level
E_o	Free energy
E_v	Valence energy
E_{FS}	Silicon Fermi energy level
E_{FG}	Graphene Fermi energy level
E_{ph}	Energy of phonon
F	Flow rate
f(ω)	Correlation coefficient
H	Coefficient of mass transport
h	Plank constant
I	Current
I_{Light}	Light current
I_{dark}	Dark current
I_D	Intensity of D band in Raman
I_G	Intensity of G band in Raman
I_{2D}	Intensity of 2D band in Raman
I_{photo}	Difference between the light and dark current
k	Wave number
K.E	kinetic energy
L_a	Average crystallite size
L_D	Average distance between point defects
M	Molarity
N	Number of graphene layers
n_D	Defect density

P	Power
P_{11}	Double resonance Raman scattering process
P_{in}	Power intensity
P_{H2}	Partial pressure of hydrogen
P_{CH4}	Partial pressure of methane
P/A	Perimeter/Area ratio
q	Wave vector
R	Resistance
r	Light reflectivity
r_{MH}	Methane to hydrogen flow rates ratio
S	Sensitivity
T	Temperature
t	time
T%	Optical transmittance
t_{fall}	Fall time
t_{rise}	Rise time
V	Voltage
W	Watt

KESAN PARAMETER PERTUMBUHAN PADA SINTESIS DAN CIRI-CIRI GRAPHENE YANG DITUMBUHKAN DENGAN APCVD UNTUK APLIKASI PENGESANAN FOTO

ABSTRAK

Graphene telah mendapat minat para penyelidik dalam tahun kebelakangan ini kerana sifatnya yang menakjubkan. Dalam kajian ini, filem graphene telah disintesis oleh teknik CVD pada tekanan atmosfera. Kesan keadaan pertumbuhan terhadap kualiti, struktur dan sifat optik telah disiasat. Kajian ini dijalankan menggunakan alat pencirian yang bersesuaian termasuk spektroskopi Raman, spektrometer UV-Vis, FESEM, dan XPS. Kajian ini mendedahkan bahawa substrat Ni menggalakkan pembentukan Gr multilapisan manakala Cu mempunyai kelebihan menghasilkan monolapisan kepada beberapa lapisan filem graphene. kajian kesan kadar aliran N_2 pada pertumbuhan graphene menunjukkan bahawa bilangan lapisan graphene, tahap kecacatan, dan kepadatan kecacatan berkurangan dengan kenaikan kadar aliran N_2. Pada kadar aliran N_2 1600 sccm, graphene monolapisan berkualiti tinggi dengan tahap kecacatan yang rendah (I_D/I_G ~ 08), $FWHM_{2D}$ yang bersesuaian ~ 29 cm^{-1} dan nisbah keamatan 2D ke G yang tinggi (I_{2D}/I_G ~ 2.4) diperolehi. Selain itu, kajian bandingan dijalankan pada kaedah pemindahan graphene termasuk pemisahan elektrokimia (ECD) dan etsa logam kimia (CME). Filem graphene yang dipindahkan oleh ECD mempunyai kecacatan/gangguan tahap terendah I_D/I_G ~ 0.05 yang membawa kepada kualiti graphene yang lebih baik. Tambahan pula, graphene telah ditumbuhkan oleh APCVD menggunakan 1-butanol sebagai cecair prekursor baru untuk karbon. Satu pengubahsuaian baru tentang prosedur pertumbuhan telah dilaksanakan. Oleh itu,

graphene monolapisan berkualiti tinggi dengan tahap kecacatan yang agak rendah (I_D/I_G ~ 0.09), $FWHM_{2D}$ yang bersesuaian ~ 34 cm^{-1} dan nisbah keamatan 2D ke G yang tinggi (I_{2D}/I_G ~ 4.85) diperolehi. Akhirnya, ciri pengesanan foto graphene/p-silikon (Gr/p-Si) pengesan foto heterosimpang mempunyai polimetil metakrilat (PMMA) sebagai lapisan penutup diselidiki. Peningkatan prestasi peranti dikaitkan dengan penggunaan lapisan PMMA/Gr sebagai lapisan antipantulan. Bagi kes pencahayaan 470 nm, nilai penambahan photodetector PMMA/Gr/ p-Si pada 5V ialah ~ 8.9 manakala masa kenaikan dan kejatuhan pada 4V berat sebelah masing ditentukan pada 0.486 s dan 0.497 s. Bagi kes pencahayaan 395 nm pada 5 V, keuntungannya ialah 9, responsif ialah 4.21 A/W dan kecekapan kuantum ialah 13.22 % manakala kepekaan pada 4 V ialah 650%. Masa kenaikan dan kejatuhan di bawah pencahayaan 395 nm pada 4V ditentukan 0.488 dan 0.448 s masing-masing.

EFFECTS OF GROWTH PARAMETERS ON THE SYNTHESIS AND CHARACTERISTICS OF APCVD GROWN GRAPHENE FOR PHOTOSENSING APPLICATIONS

ABSTRACT

The graphene has gained a tremendous interest of researchers in recent years due to its amazing properties. In the present work, graphene films have been synthesized by the CVD technique at atmospheric pressure. The effects of growth conditions on the quality, structural and optical properties were investigated. The study was carried out using appropriate characterization tools including Raman spectroscopy, UV-Vis spectrometer, FESEM, AFM, and XPS. The study revealed that the Ni substrate promotes the formation of a multi-layered graphene whereas the Cu has the advantage of producing mono to few-layered graphene films. Studying the effect of the N_2 flow rate on graphene growth showed that the graphene layers number, defects level, and defect density decreased by the increment of the N_2 flow rate. At N_2 flow rates of 1600 sccm, high-quality monolayer graphene with relatively low defects level (I_D/I_G ~08), appropriate $FWHM_{2D}$ ~ 29 cm^{-1} and high 2D to G intensities ratio (I_{2D}/I_G~ 2.4) were obtained. Besides, a comparative study was conducted on graphene transfer methods including electrochemical delamination (ECD) and chemical metal etching (CME). The graphene film which was transferred by ECD has the lowest defects/disorder level I_D/I_G ~ 0.05 that led to better graphene quality. Furthermore, graphene was grown by atmospheric pressure chemical vapor deposition (APCVD) method using 1-butanol as a new liquid precursor for carbon. A new modification on the growth procedure was implemented. Thus, high-quality monolayer graphene with

relatively low defect level (I_D/I_G ~0.09), appropriate $FWHM_{2D}$ ~ 34 cm^{-1} and high I_{2D}/I_G~ 4.85 were obtained. Finally, the photodetection characteristics of graphene/p-silicon (Gr/p-Si) heterojunction photodetector having Polymethyl Methacrylate (PMMA) as the cladding layer was investigated. The enhancement of device performance is attributed to the use of a PMMA/Gr layer as an antireflection layer. For the case of 470 nm illumination, the gain value of the PMMA/Gr/p-Si photodetector at 5V was ~ 8.9 while the rise and fall times at 4V bias were determined to be 0.486 s and 0.497 s respectively. For the case of 395 nm illumination at 5 V, the gain was 9, the responsivity was 4.21 A/W and the quantum efficiency was 13.22 % while the sensitivity at 4 V was 650%. The rise and fall times under 395 nm illumination at 4V were determined to be 0.488 s and 0.448 s respectively

CHAPTER 1

INTRODUCTION

1.1 Introduction

Since the discovery of graphene in 2004 until today, studies are continuing to benefit the remarkable characteristics of graphene in various real-world applications. The graphene structure consists of carbon-carbon sp^2 bonds that combine to form a hexagonal lattice of one atom thickness. Due to its nanoscale thickness, which is smaller than the size of electron wavelength, graphene is considered as a 2D nanostructure. Graphene has gained a tremendous interest of researchers in recent years due to its amazing properties. Graphene can be considered as a perfect transparent electrode as compared to the other materials due to its higher light transmittance (97.7%) and electrical conductivity [1]. Besides, it has high mechanical strength with a large Young's modulus (130 Gpa) and high flexibility. The high mobility (200,000 $cm^2\ V^{-1}\ s^{-1}$) of graphene makes it a superior material in the high-speed electronic devices [2, 3]. These properties have emerged graphene as the best candidate for use in electronic and optoelectronic applications such as the field-effect transistors FETs, supercapacitors, organic LEDs as well as the photodetectors.

Graphene can be produced by several methods such as mechanical exfoliation, electrochemical exfoliation, direct graphite sonication, graphene oxide (GO) reduction, epitaxial growth and chemical vapor deposition (CVD). Among these methods, the CVD technique is found to be quite useful to produce high quality and large size graphene films [2-4]. The CVD is commonly recognized to include the carbon source decomposition with the assistance of heat and metallic catalysts. Adjusting the growth conditions such as, growth temperature, carbon precursor types, carbon precursor flow rates, as well as the choice of catalytic substrates on which graphene is deposited,

contribute in improving the graphene quality. The change in temperature usually changes the defects level and the graphene thickness and also plays an important role in changing the crystallite size. Ethanol, methanol and butanol carbon precursors are safe and low-cost liquid carbon precursor as compared to methane. Controlling the reactant gases flow rates, including hydrogen and inert gases, is a common practice in graphene production to control the graphene properties. Several studies for graphene synthesis were performed using various transition metals, including Cu, Ni, Pt and many others [5-8]. These studies indicated that the graphene is formed by two different mechanisms based on the magnitude of the carbon solubility in these metals. Low-carbon-solubility metals follow the surface mechanism, while the high-carbon-solubility metals follow the segregation process. The fact that graphene is exploited in various applications, it must be transferred onto various substrates such as polymers, oxides, and other substrates.

Due to its possible use in optoelectronic applications graphene has gained significant interest from researchers [9-13] . Graphene is capable of confining electromagnetic energy to nano-scaled volume and tuning the optical properties by electrical gating[14, 15]. It has a low energy dissipation rate and exhibits high mobility and concentration of carriers. In fact, graphene has a steady optical absorption for a wide spectrum ranging from infrared (IR) to ultraviolet (UV) spectra. Because of these unique properties, graphene is preferable to many other materials for photodetection.

1.2 Problem Statement

Graphene is a promising material for advanced electronic applications. There are many methods to produce graphene, including chemical vapor deposition CVD. Graphene growth by CVD is carried out at different pressure conditions, including ultra-high vacuum (UHV), low pressure (LPCVD), and atmospheric pressure (APCVD) [16]. The production of graphene under atmospheric pressure eliminates the need for costly vacuum pumps and reduces energy consumption. Besides, this method limits copper sublimation at high growth temperatures and thus reduces the contaminations of the quartz tubes that is used in graphene synthesis systems[17, 18].

Production of graphene using CVD is carried out using various carbonic precursors, including gas, liquid, and solid [19]. The use of liquid carbonic precursors is distinguished from the other as being safe, non-explosive, and less expensive. Moreover, the use of these liquid precursors facilitates the graphene doping process as compared to the gaseous or solid precursors. According to previous studies, many liquid carbonic precursors were used to produce graphene such as methanol, ethanol, and benzene at different growth conditions. Studies demonstrated that the produced graphene films were impacted by the type of carbon precursors used. For instance, graphene domains with larger crystallite size (*La*) can be obtained using methanol precursor as compared to ethanol and propanol [20]. Thus, research on new liquid carbon precursors to produce graphene is useful and promising.

The study aims to use 1-butanol (C_4H_9OH) as a liquid carbon source to produce graphene at atmospheric pressure conditions. 1-butanol has the advantage of being less productive for polluting gases such as carbon dioxide and carbon monoxide as compared to other precursors such as benzene, ethanol, and methanol[21].

Graphene is extensively used in electronics, especially optoelectronic applications. Graphene growth conditions are often adjusted to obtain better optical and electrical properties. The growth conditions are multiple include temperature, substrate type, carbon source type, as well as flow rates of reaction gases. So, adjusting the growth conditions and producing graphene film by APCVD using liquid precursors is a promise for the industrial scale. The properties of graphene as a conductive and transparent material, makes it suitable to be used with other semiconductors such as silicon [9-11]. Thus, the study aims to use graphene (Gr) with p-type silicon(p-Si) substrates to fabricates a Gr/p-Si heterojunction photodetector. The study also looks to improve the performance of the Gr/p-Si photodetector by adding PMMA as a cladding layer that can reduce the light reflectivity.

1.3 Study Objectives

1- To explore 1-Butanol as a potential liquid precursor for graphene synthesis via APCVD.

2- To study the optical and structural properties of the APCVD grown graphene under the effects of different growth conditions such that (i) using copper (Cu) and nickel (Ni) as catalytic substrates at various ethanol flow rates (ii) applying various nitrogen flow rates at constant methanol flow rate using Cu substrate.

3- To study the effect of the transfer methods including the electrochemical delamination and chemical metal etching techniques on the structural and optical properties of graphene.

4- To evaluate the photodetection characteristics of Gr/p-Si heterojunction photodetector having PMMA as a cladding layer

1.4 Originality

The originality of this work appears in several aspects which can be summarized as follows:

1- The 1-butanol was utilized as a new potential liquid precursor for graphene synthesis via APCVD. A new experimental procedure was also implemented to produced graphene even at low flow rate of butanol.

2- The impact of the nitrogen gas flow rate on the CVD grown graphene especially on Cu foils has been rarely studied. In this work, more details for the effects of nitrogen gas flow rates on graphene characteristics were investigated.

3- In previous studies, the Gr/PMMA layer was used on silicon dioxide/silicon (SiO_2/Si) substrate for use in the gas sensors that can detect the volatile organic compounds. However, to our knowledge, this is the first time that a PMMA/Gr layer has been used to enhance the light-sensing properties of a Gr/p-Si heterojunction photodetector by two-step fabrication.

1.5 Thesis Outlines

This work consists of six chapters: the first chapter includes an introduction to the work, the problem statement and the objectives of this project through which the problem can be addressed. In the second chapter, the study aims to highlight the most important work and previous research in this area, including methods of production of graphene and growth conditions of CVD technique as well as the transfer methods. The fundamentals of graphene structures including monolayer, double-layer, few-layer, and even the graphite structure is also briefly reviewed. The semantics of Raman spectra and their precise analyses are explained. The most important characteristics of photodetectors and the mechanisms of graphene/silicon Schottky heterojunctions were then presented.

The experimental procedure chart, pre-growth treatments, the CVD growth system, transfer methods, the characterization tools and the photodetector design methods are presented in chapter three. Chapters 4 showed and explained the results of various growth conditions on the structural, morphological, and optical properties of graphene. The results regarding the use of butanol as a new source of graphene production were reviewed and justified. The results of graphene transfer by different methods were reviewed and compared in this chapter. The Raman spectra, UV-vis measurements, and the FESEM images were the main data that were discussed in this chapter. Chapter 5 shows how graphene was employed in photodetectors applications. The design and mechanisms, as well as the photodetection characteristics of the PMMA/Gr/p-Si photodetector were demonstrated. Finally, the main conclusions of the study were outlined in chapter 6. A vision of what can be done in this broad field in the future was also presented.

CHAPTER 2

LITERATURE REVIEW & THEORETICAL BACKGROUND

2.1 Introduction

In this chapter, a theoretical background is presented concerning the crystal structure of graphene as a two-dimensional material and as a basic material for other carbon structures. Electronic-band-structure for single- and bi-layer graphene are also indicated. The optical properties of graphene and their relation to the number of layers are illustrated. Some well-known methods of graphene production, especially chemical vapor deposition, were reviewed. It was then shown how to analyze the Raman spectra of graphene. Finally, photodetection characteristics, especially for graphene/silicon photosensors, were reviewed.

2.2 Graphene Theoretical Background

The study of the graphene field delivered a sudden jerk since 2004 when Andre Geim and Konstantin Novoselov first isolated mono-layer graphene from graphite [22]. This event was surprising since the two-dimensional crystals were unstable at a certain temperature according to the Peierls and Landau Thermodynamic law [22, 23].

The graphene structure consists of carbon-carbon sp^2 bonds that combine to form a hexagonal lattice of one atom thickness. Due to its nanoscale thickness, which is smaller than the size of electron wavelength, graphene is considered as a 2D nanostructure. Graphene has gained a tremendous interest to researchers in recent years due to its amazing properties (Table 2.1). It was found that the significant reduction in the electronic shielding effect can substantially change the many-particles-interactions in the 2D-materials as compared to their bulk structures. This leads to the emergence of unique properties in 2D-materials. For example, the Fermi energy of electrons/holes in

2D-materials is directly proportional to the carrier charges number n while for bulk materials it depends on $n^{2/3}$ [24]. For graphene, the unique properties involve the linearity in energy dispersion relation and the approximately zero mass carriers [1, 25, 26]. Furthermore, graphene can be considered as a perfect transparent electrode as compared to the other materials due to its higher light transmittance (97.7%) and electrical conductivity [27]. In addition, it has high mechanical strength with a large Young's modulus (130 GPa) and high flexibility. When considering infinitesimal thickness, graphene can be considered as the strongest material that ever measured [28]. The high mobility of graphene (200,000 $cm^2\ V^{-1}\ s^{-1}$) which is higher than that of advance material such as carbon nanotube (100,000 $cm^2\ V^{-1}\ s^{-1}$) and crystalline silicon (1400 $V^{-1}\ s^{-1}$)[29, 30] . Thus, graphene can be considered as a superior material in the high-speed electronic devices.

Graphene is produced by several methods such as mechanical exfoliation, electrochemical exfoliation, direct graphite sonication, GO reduction, epitaxial growth and chemical vapor deposition (CVD). Among these methods, the CVD technique is found to be quite useful to produce high quality and large size graphene films [2, 31]. The CVD is commonly recognized to include the carbon source decomposition with the assistance of heat and metallic catalysts. The graphene layers pinned to the substrate by the van der Waals force and could be released as free-standing graphene. Adjusting the growth conditions such as, the growth time, growth temperature, carbon precursor types, reactant flow rates, as well as the choice of catalytic substrates on which graphene is deposited, contribute to improving the graphene quality [3, 32, 33].

Table 2.1. Graphene Properties

Graphene properties	Value	Reference
Crystal structure	Hexagonal	[3]
Interlayer spacing	0.34 nm	[3]
Electrical conductivity	4 e^2/h $(\Omega.m)^{-1}$	[3]
Energy gap	~ 0 ev	[3]
Thermal conductivity	5000 W/mK	[34]
Young's modulus	130 Gpa	[3]
Charge carrier mobility	200,000 cm^2 V^{-1} s^{-1}	[34]
Optical transmittance	97.7 %	[22]
Melting point	4510 K	[35]
Specific surface area	~ 2630 m^2/g	[34]

2.2.1 Graphene as the primary structure of other carbon allotropes

The graphene structure consists of carbon-carbon sp^2 bonds that combine to form a hexagonal lattice of one atom thickness. The separation between the two most neighbour carbon atoms in graphene lattice is a_o ~1.42 Å. For multi-layered graphene, the separation between two consecutive vertical planes is ~ 0.34 nm. The unit cell of graphene has two inequivalent carbon atoms A and B each of them is surrounded by three atoms as nearest neighbours arranged in an equilateral triangle. Typically, the graphene lattice is divided into 2 sublattices each of them takes the shape of the equilateral triangle denoted as sub-A with basis atom A and sub-B with basis atom B. The two sublattices can be considered as Bravais lattices (Figure 2.1(a)). The primitive lattice vectors $\mathbf{a_1}$ and $\mathbf{a_2}$ are given by equations (2.1a) and (2.1b) respectively [36].

$$\mathbf{a_1} = a\left(\frac{1}{2}, \frac{\sqrt{3}}{2}\right) \tag{2.1a}$$

$$\mathbf{a_2} = a\left(\frac{1}{2}, \frac{-\sqrt{3}}{2}\right) \tag{2.1b}$$

Herein, a ~ 2.46 Å is the graphene lattice constant. The first Brillouin-zone of graphene in reciprocal space has a hexagonal shape as can be shown in Figure 2.1(b). The primitive-reciprocal-vectors $\mathbf{b_1}$ and $\mathbf{b_2}$ are pointed out in the figure. The high-symmetry degeneracy points K and K′ (also known as Dirac points) can be observed at hexagonal corners, as well as other high-symmetry points Γ and M. The Dirac points K and K′, are the locations of Dirac cones tips that appear in (E-k) dispersion relation. According to the orthonormal relations between real and reciprocal primitive vectors in the 2D lattice ($\mathbf{a_i}.\mathbf{b_j} = 2\pi\,\delta_{ij}$), the primitive reciprocal vectors $\mathbf{b_1}$ and $\mathbf{b_2}$ in term of a can be written as follows:

$$\mathbf{b_1} = \frac{2\pi}{a}\left(1, \frac{1}{\sqrt{3}}\right) \tag{2.2a}$$

$$\mathbf{b_2} = \frac{2\pi}{a}\left(1, \frac{-1}{\sqrt{3}}\right) \tag{2.2b}$$

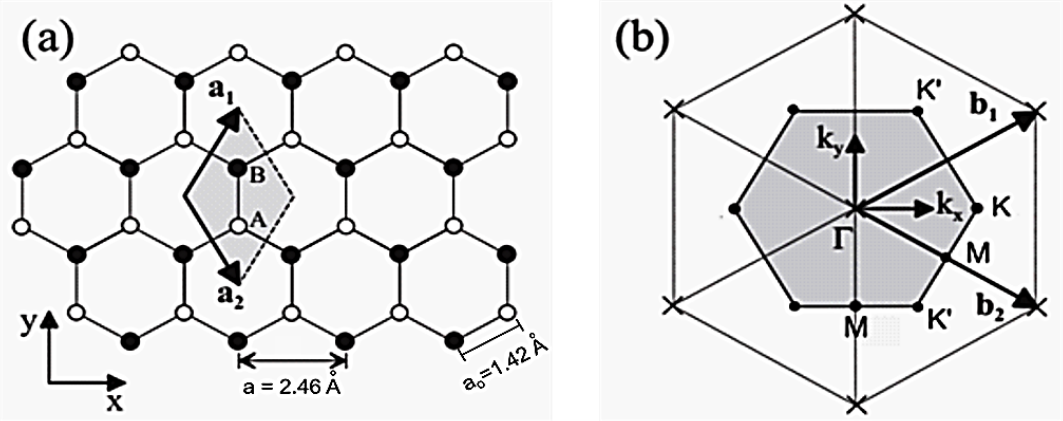

Figure 2.1. The hexagonal graphene lattice (a) in real space and with primitive vectors $\mathbf{a_1}$ and $\mathbf{a_2}$. The unit cell is represented by the grey rhombus. (b) the first Brillouin-zone with the reciprocal lattice vectors $\mathbf{b_1}$ and $\mathbf{b_2}$ in momentum space [36].

The strong covalent bonds between the in-plane carbon atoms were formed by the hybridization of 2s and 2p orbitals producing sp^2 state. However, the weak Van der Waals interactions between two vertical planes give the slippery property of graphite

layers. Graphene can be considered as the primary structure of many carbon forms such as carbon nanotube, fullerenes, and graphite. As shown in Figure 2.2 graphene (Gr) is a fundamental building block for the other graphitic materials. The 0-dimensional (0D) fullerene can be formed by wrapping a graphene sheet that has a specific number of pentagon carbon rings. The 1-dimensional (1D) single or multi-walled carbon nanotubes (SWNTs and MWNTs) is obtained by rolling the graphene sheet whereas the 3-dimensional (3D) graphite is elevated through the vertically stacking of the graphene layers [22, 27].

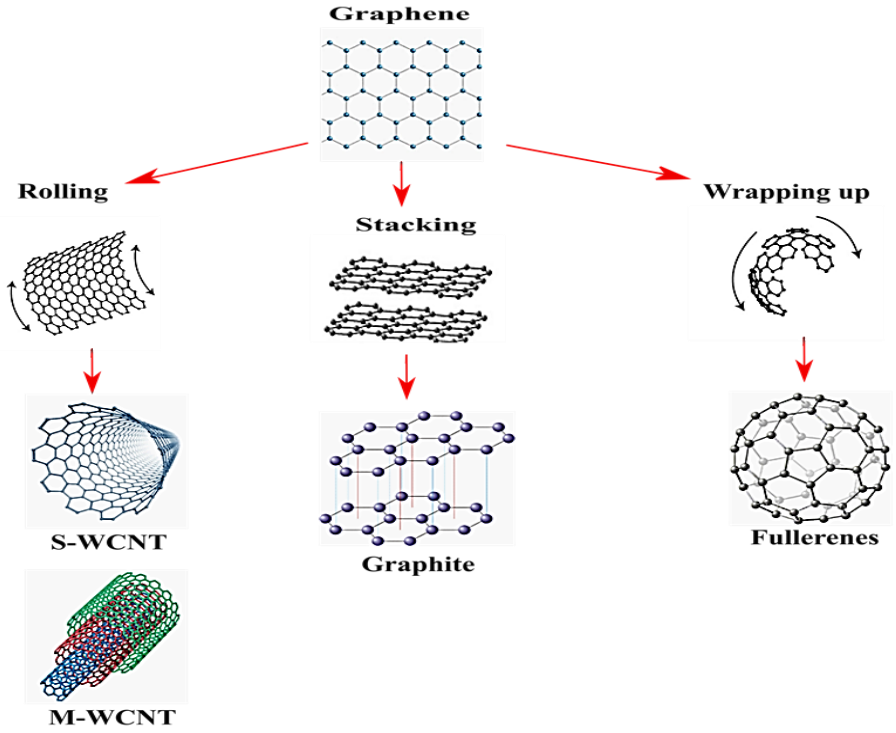

Figure 2.2. Graphene (Gr) as a fundamental building block for the other graphitic materials including S-WCNT, M-WCNT, graphite and fullerene.

The bilayer graphene is a structure that consists of two parallel sheets stack vertically. The Bernal or the AB-stacked form is the most common arrangement of bilayer graphene. In this stacked form, half the number of carbons in the top layer

positioned above the centres of the empty hexagons in the bottom layer. Figure 2.3(a) shows Bernal-stacked form in which the carbon atom A_2 in the top layer locates above the carbon atom B_1 in the bottom layer. Figure 2. 3(b) shows the tri-layer graphene which contains bilayer graphene with Bernal stacking as the first two layers and monolayer graphene as the third layer. The A_3 carbon atom in the third layer locates above the A_1 atom in the first layer while B_3 locates above B_1. The graphite is a 3D structure that is constructed by the vertically stacking of the individual layers of graphene [37].

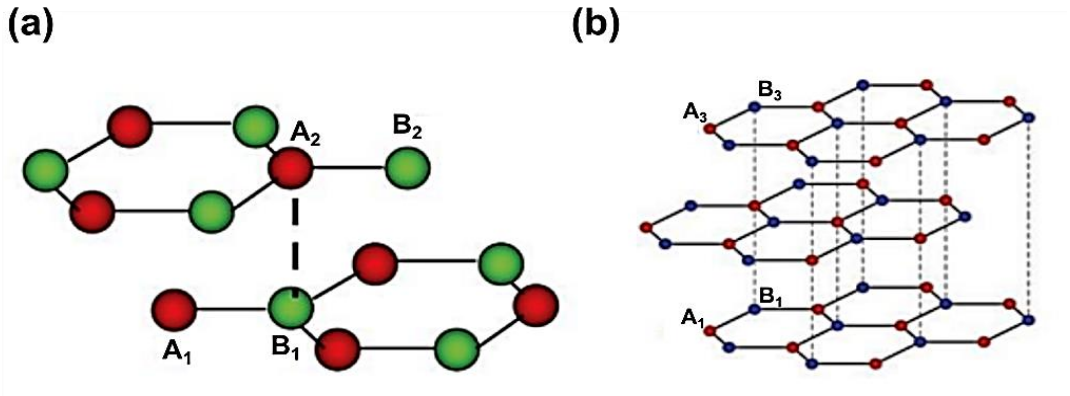

Figure 2.3. (a) Bilayer graphene structure of Bernal-stacked form (b) tri-layer graphene of ABA-stacked form [38]

2.2.2 Graphene edges

Graphene domain terminals exhibit two types of edges that are the armchair and the zigzag edges. They can be determined according to the orientation of the hexagons relative to terminal length (Figure 2.4). It's worth to mention that the graphene structure with zigzag edges is more stable than armchair one according to Raman analysis. The graphene domains that have armchairs edges exhibit strongly higher D-band intensity compared to the zigzag edges[39].

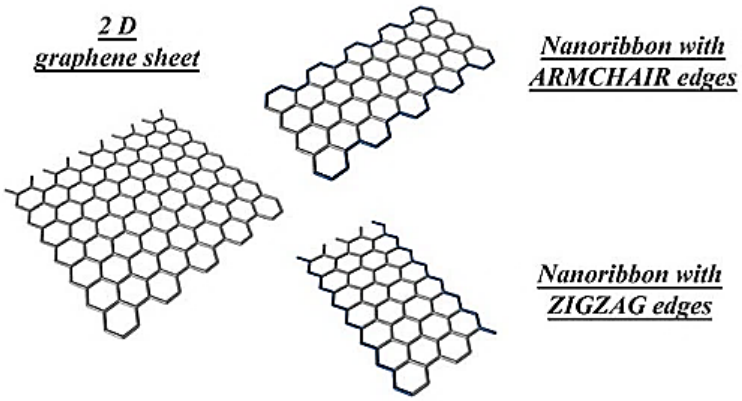

Figure 2.4. Armchair (up) and zigzag (down) edges in graphene nanoribbons[40].

2.2.3 sp^2 hybridization

Graphene is a hexagonal net of carbon atoms that bond together through the sp^2 hybrid bonds. Each carbon atom has 6 electrons involving 2 core electrons and 4 valence electrons distributed in their orbitals as follows $1s^2\ 2s^2\ 2p_x^1 2p_y^1\ 2p_z$.

The sp^2 hybridization process takes place as the 2*s* orbital combine with $2p_x$ and $2p_y$-orbitals to form the trigonal planer of sp^2orbitals. The remainder unhybridized p_z-orbital is perpendicular to the centre of trigonal planer sp^2 assemblage. Each sp^2-orbital can combine with other sp^2-orbital to form a strong covalent bond known as σ-bond. The angle between any two σ-bonds is 120°. The new electron distribution of the graphite carbon atom after the hybridization process is $1s^2\ (sp^2)^1\ (sp^2)^1\ (sp^2)^1\ 2p_z^1$ (Figure 2.5(a)). In graphene lattice, the electrons of p_z-orbitals of the neighbour carbon atoms can share to form π-bonds. Each carbon atom in graphene lattice has three first-neighbour atoms and thus binds with each neighbour by $1\frac{1}{3}$ bond as shown in Figure 2.5(b). For the multilayer graphene, the weak interaction between the stacked layers is due to Van-der-Waals-forces which are reduced by the impact of π-orbitals. For the band structure of graphene and graphite, the overlapping of p_z-orbitals at Dirac points (K-points at the first-Brillion-zone in the reciprocal space of graphene lattice) leads to

the formation of valence and conduction bands that known as the bonding π and anti-bonding π* bands respectively (Figure 2.5(c)) [41].

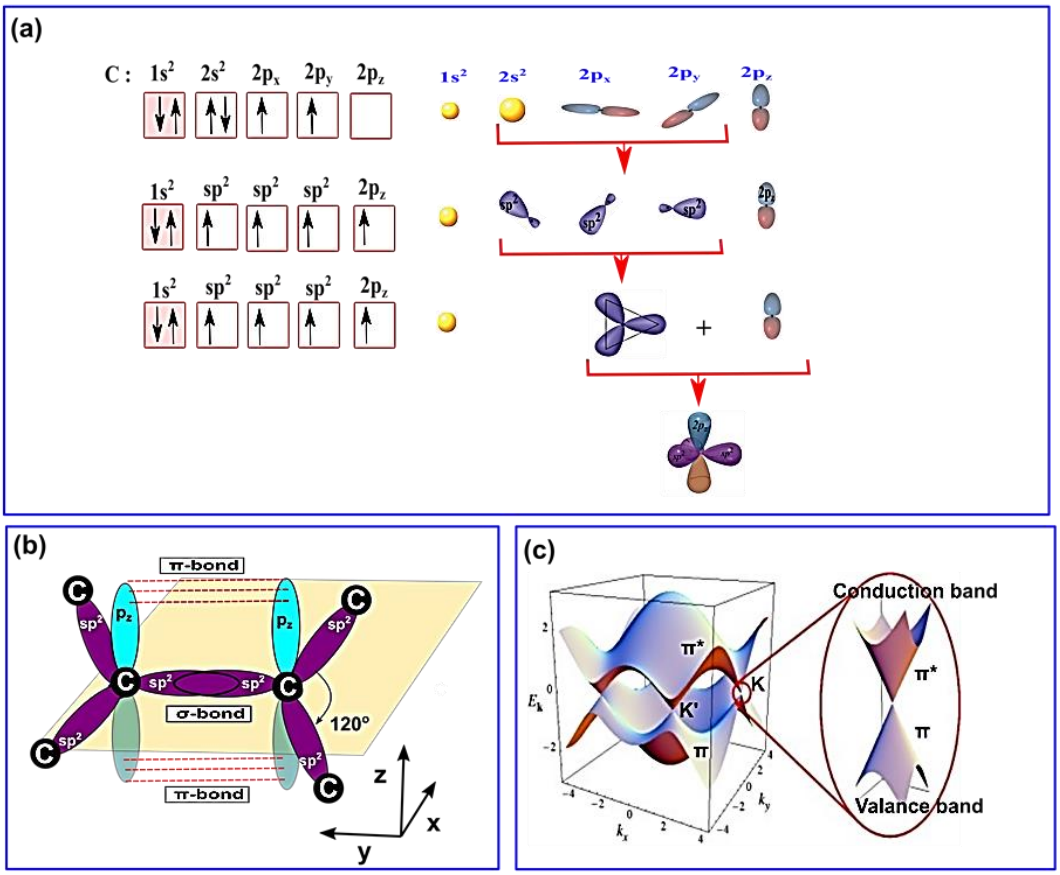

Figure 2.5. (a) The sp^2 hybridization process (b) carbon atom in graphene lattice has three first- neighbour atoms and thus bound with each neighbour by $1\frac{1}{3}$ bond (c) band structure of graphene.

2.2.4 Band Structure of Mono and Double Layers Graphene

Most of the optical microscopies depend on light interference to identify graphene sheets. Unfortunately, this method could not determine the graphene layers number. The thickness of graphene film is a fundamental character that impacts other graphene properties. The amazing mechanical strength of graphene is due to the covalent strong σ-bonds between the carbon atoms in the hexagonal structure. The unique band structure of graphene is mainly related to the π -bonds. As can be observed

in Figure 2.6(a), the valance and conduction bands meet into conical sharp contacts at six symmetric points located at the corners of the Brillouin-zone.

Researchers typically interested in a very small energy limit near the bands touching points (Dirac points) because of the amazing and exciting characteristics of graphene are achieved at these limits. At Dirac points (K and K′), the band structure of graphene is linear according to the Dirac equation (see equation 2.3). Furthermore, the effective mass ~ zero near these Dirac points. The linear- band-structure of graphene with a gapless energy band at Dirac points resulted in semimetal or semiconductor material behaviour. Electrons behave as relativistic massless particles (Dirac fermions) near Dirac points and subject to the Dirac equation.

$$E(k) = v_F \hbar k \tag{2.3}$$

In which v_F refer to the Fermi speed of massless particles ~ 1×10^6 ms^{-1}, and k is the magnitude of wavenumber. As shown in Figure 2.6(b), the existence of the energy gap in the double-layers graphene structures depends on its symmetry. In the symmetric structure, there is no energy gap as well as the monolayer structure. In contrast, the asymmetric double layers graphene possesses this gap. However, the gapless energy band can be opened by applying a perpendicular electric filed to the graphene lattice, which in turn, can break its symmetry (Figure 2.6(c)). For multilayers graphene the band structure is different, and the energy gap is not zero. This is because the stacking of further layers makes the electrons/holes wave functions overlap leading to metallic overall behaviour. Thus, the identification of layers number is an urgent necessity[22, 42, 43].

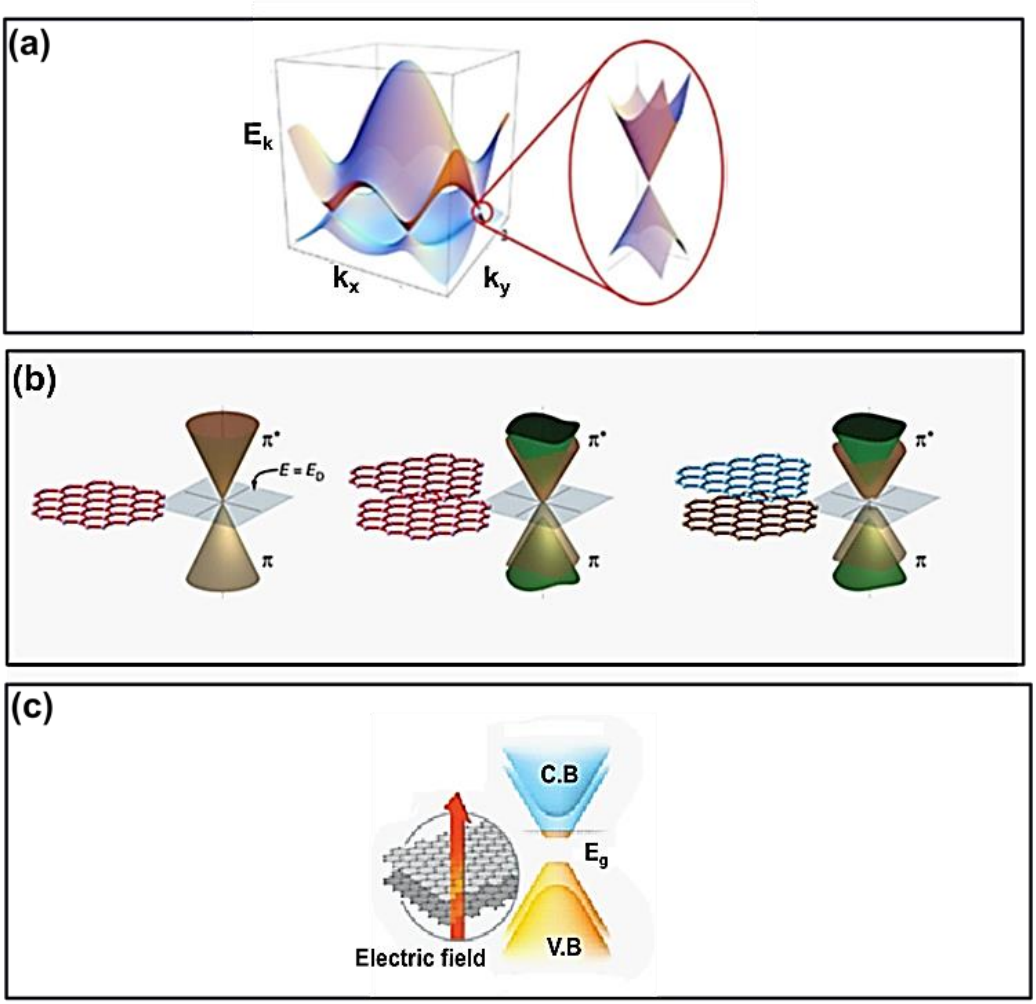

Figure 2.6. (a) Graphene band structure. The magnifier section shows the valence and conduction bands near Dirac points. (b) Electronic structure of monolayer, symmetric bilayer and asymmetric bilayer from left to right respectively (c) The applying of an electric field to the symmetric bilayer graphene can open its energy gap [43-45].

2.2.5 Optical Properties of Graphene

UV-Vis measurements can be performed to estimate the number of graphene layers. Thus, the visible light transmittance of the studied samples should be measured. Ideally, the visible light absorption of the monolayer graphene sheet is given by πα~2.3%, where $\alpha = 1/137$ is the fine structure constant [46]. Thus, the optical

transmittance of monolayer graphene is T~ 1- πα =97.7% as can be seen in Figure 2.7. Worth to mention that the reflectance of monolayer graphene is very small ~ 0.1%.

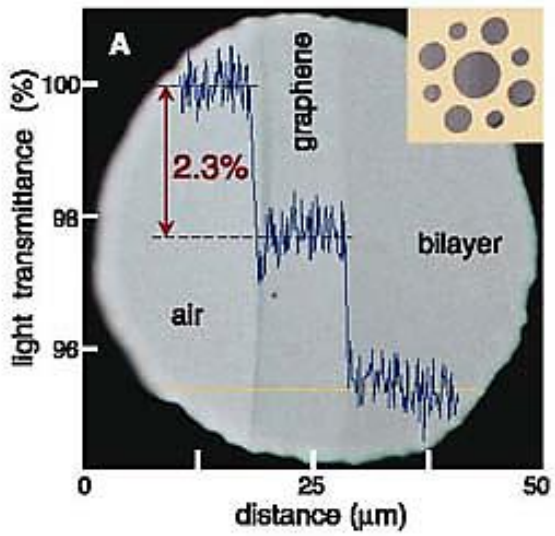

Figure 2.7. The visible light absorption of the monolayer graphene sheet is ~2.3%. The optical transmittance of mono and bilayer graphene can be observed [46]

However, relying solely on πα would be insufficient to determine the number of graphene layers accurately, since optical absorption due to residue PMMA (that is used in graphene transfer process) as well as stacking effects from multilayer graphene affects the overall transmittance. Hence, other parameters such as universal optical conductance can be employed to improve upon the accuracy [47, 48]. Consequently, transmittance, $T(\omega)$, of stacked graphene can be expressed according to equation (2.4) [47]:

$$T(\omega) = \left[1 + \frac{f(\omega)\pi\alpha N}{2}\right]^{-2} \tag{2.4}$$

Where $f(\omega)$ is the correlation coefficient; N is the number of graphene layers. To eliminate the optical changes due to graphene stacking, the transmittance at 550 nm light source would be used. There, $f(\omega)$ was determined to be 1.13 [47]. By

compensating the values of $f(\omega)$ and α, N as a function of T can be written as in equation (2.5).

$$N = \left[\frac{T^{-0.5} - 1}{0.0129385} \right] \tag{2.5}$$

2.3 Graphene Production Methods

Since the advent of graphene to this day, there have been many versatile techniques for graphene production which include mechanical and chemical exfoliation, graphene oxide reduction, graphene pyrolysis, epitaxial growth, thermal and plasma-enhanced CVD, arc-discharge method, the spray method, and many others[4]. However, in this section the some of the most common methods will be addressed as follows:

2.3.1 The Peeling Method

Removing the graphene layer from ultra-high purity graphite bulk using scotch-tape, then pressing the tape down against an appropriate substrate to deposit a layer of graphene known as the peeling method [3]. The layers present on the scotch-tape have much thickness than monolayer but when the tape is lifted, a graphene monolayer remains on the substrate by the Van der Waals attraction force (Figure 2.8(a)).

2.3.2 Graphene Production by SiC Sublimation

In this method, the silicon carbide SiC wafer is annealed at high temperature ~ 1000-1200^{o}C, and consequently, the top layer of SiC would be thermally decomposed meanwhile the Si atoms would sublimate. The remaining carbon can be re-bonded and rearranged to form graphene film (Figure 2.8(b)) [49, 50].

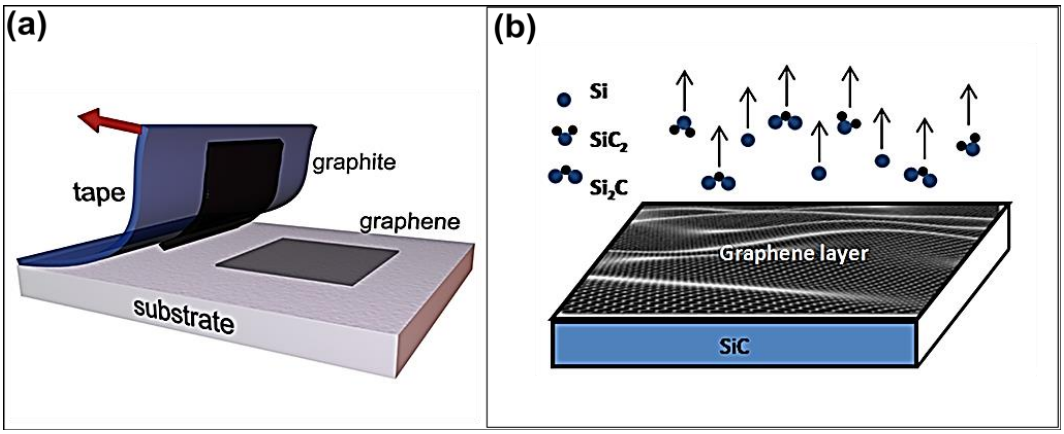

Figure 2.8. Graphene growth methods (a) The peeling method (scotch tape method) (b) The sublimation of SiC [51].

2.3.3 Electrochemical Exfoliation of Graphite

The electrochemical exfoliation technique is an efficient and promising approach for graphene production using graphite. In such a technique, an electrical voltage is applied to drive the cations/anions to insert into graphite causing the formation of gaseous species and thus the graphene sheets can be expanded and exfoliated as individual layers. As shown in Figure 2.9(a), the electrochemical cell consists of electrolyte solutions (acidic solution such as H_2SO_4), graphite as working electrode and Pt as the counter electrode. The graphite electrode is connected to positive voltage (+7 to 10V) while the Pt electrode is connected to the negative terminal. The exfoliation process will be completed after a few minutes (Figure 2.9(b)) where the exfoliated material is then collected using vacuum filtration. Subsequently, the collected powder can be repeatedly washed by water and afterward dispersed in N, N-dimethylformamide (DMF) to produce exfoliated graphene layers (Figure 2.9(c, d)). Several factors control the efficiency of the exfoliation process to determine the produced percentage of the exfoliated graphene and the most prominent factors are : (i) the concentration of electrolyte solution, (ii) the applied voltage to the electrochemical cell and (iii) the exfoliation time[3, 52, 53].

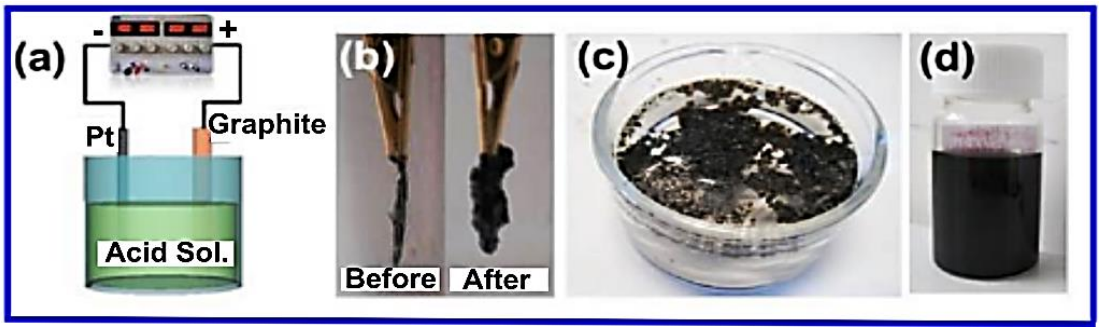

Figure 2.9. (a) the electrochemical cell schematic illustration, (b) the graphite electrode before (left) and after (right) electrochemical exfoliation, (c) exfoliated graphene floats in water, (d) dispersed graphene flakes in DMF[53].

2.3.4 Reduced Graphene oxide (r-GO)

Graphene oxide has a layered structure as of graphite, but its carbon planes are connected with oxygen-containing groups(O-CGs) that permeate the carbon layers. This not only increases the spacing between successive planes but also makes them hydrophilic. GO as layers can be peeled in water by a moderate ultrasonication process. Thus, the GO layers can be reduced to obtain perfect graphene due to the elimination of O-CGs associated with the carbon layers.

The reduction methods can be classified into three main categories, the thermal, chemical and multistep reductions. The thermal reduction can be subdivided into (i) thermal annealing and (ii) thermal irradiation, while the chemical reduction can be classified into (i) chemical reagent reduction, (ii) photocatalyst reduction, (iii) electrochemical reduction and (iv) solvothermal reduction. Despite several attempts that have been made to make graphene oxide features similar to that of graphene, this is difficult to achieve due to the presence of residues in the form of functional groups and structural defects at the carbon planes.

To date, the Hoffman and Hummers methods are being used to prepare graphene oxide. In this method, the graphite is subjected to the oxidation process by treating it

with a chemical mixture of sodium nitrate, potassium permanganate and concentrated sulfuric acid without water. The carrier mobility and carrier concentration are low in graphene oxide due to the presence of the functional groups that break the symmetry of the graphitic lattice structure and limit the transition of π-electrons. Thus, the GO has a large sheet resistance of 10^{12} $\boldsymbol{\Omega}$/sq, which causes it to act as an insulating material. Based on the above, the reduction of GO will not only contribute to the removal of oxygen containing-groups and lattice defects but also helps to recover the conjugated-network-of-the-graphitic-lattice. After the GO reduction process, the reduced graphene oxide (r-GO) can be distinguished by several criteria including: (i) the r-GO exhibits black colour after the chemical reduction instead of yellowish brown colour for the case of GO (Figure 2.10), (ii) the r-GO electrical conductivity is much higher as compared to GO, (iii) the r-GO has significantly lower oxygen to carbon ratio (O/C) as compared to GO case. However, other analysis techniques can be used to obtain more details about the structural aspects and other properties of GO and r-GO such as Raman spectroscopy, atomic-force-microscopy (AFM), transmission-electron-microscopy (TEM) and solid-state FT-NMR spectroscopy [54].

Figure 2.10. The r-GO exhibits black colour after the chemical reduction instead of yellow–brown colour for the case of GO[54].

2.4 Chemical Vapor Deposition (CVD)

The study of graphene growth conditions by the chemical deposition method has attracted the interest of researchers to obtain high-quality graphene films that are suitable for different enormous applications. In this section, these conditions will be reviewed consistently from the use of different metal catalysts to the exploitation of different carbon sources for graphene synthesis. The most commonly used carbon precursor for graphene growth is methane. There are different sources also used including; gas, liquid, and solid precursors. However, the use of liquid sources has the advantage to facilitate the graphene doping process by using organic solvents containing proper elements such as nitrogen(N) or boron(B). The most common catalysts substrates used for graphene growth are Cu and Ni. The thickness of the Cu used is between 25 and 50 μm. Most of the reports indicated that the graphene was grown at 1000 ℃ but growth at various temperatures was also reported. In some reports, the pressure values used for growth ranged between 1 and 50 Torr and at atmospheric pressure. Mixtures of gases involving; hydrogen, methane, and an inert gas such as argon or nitrogen at different ratios have been reported. In addition, other factors affecting graphene growth include growth time and substrates treatment were studied [19, 55, 56].

2.4.1 Transition Metals Substrates

Reports indicate that multi-layers graphene (graphite) were deposited on transition metals for five decades. The formation mechanisms in which the carbon can be combined with some other materials to be decomposed to produce graphite were reported in 1896 [57, 58]. Afterward, the graphite growth on the Pt substrate was reported. The study revealed that the carbon radicles were firstly diffused onto the metal surface through the annealing process then they were segregated from the bulk to Pt

surface via cooling to produce graphite film [59]. Graphene could be grown by CVD on various transition metal substrate including; copper (Cu), nickel (Ni), rubidium (Ru), Iron (Fe), platinum (Pt), palladium (Pd) or Cobalt (Co), Rhenium (Re) or other metals [60].

The CVD approach considers inexpensive, accessible and promises for advanced devices compared to other methods. Many previous studies proved the excellent performance of devices that were fabricated using the graphene which was grown on Cu by CVD technique [61]. The selection of copper as a preferred substrate is due to the low solubility of carbon toward copper as compared to other metals. However, the carbon solubility toward transition metal substrates plays a key role in determining the growth mechanism.

Recently, Cu and Ni were exploited to optimize the growth conditions to produce a large area with high-quality CVD grown graphene. After the growth, graphene film is transferred onto dielectric substrates. The previous study indicated that the mobility of graphene that was deposited onto the Ni substrate and subsequently transferred onto the SiO_2/Si substrate was around 3650 $cm^2 V^{-1}s^{-1}$ [60]. One of the main limitations of using Ni as a catalyst substrate for graphene growth is the heterogeneous coverage (uneven layers distribution) along the substrate surface. The difficulty in controlling the homogeneity of graphene layers is attributed to the difference in cooling rates between grains and grains boundaries of Ni substrate. The carbons segregation rapidly occurs along the grains region while the cooling is heterogeneous at the grain boundaries [62, 63]. In contrast, a higher uniformity deposition of large-scale monolayer graphene with high quality could be produced using Cu as a catalyst substrate. For instance, the growth of monolayer graphene of large area ~ 30-inch has been reported. According to Raman spectroscopy measurements and imaging details of

advanced microscopies, 95% coverage on Cu surface was achieved for monolayer graphene while the rest percentage was achieved for two or three layers [64] .

2.4.1(a) Why Copper Substrate?

The graphene films deposited on Cu surface are subjected to surface interaction mechanism for several reasons including (i) C solubility in Cu is low, (ii) C-Cu interaction is weak, (iii) low energy barrier of C diffusion on Cu-surface. These factors also clarify why Cu is preferable for producing monolayer graphene films. Furthermore, the low diffusion energy barrier of C on the Cu surface explains the high mobility of C atoms along Cu-surface which can freely travel and join to existing graphene domains. Furthermore, the surface mobility of surficial Cu atoms increases at high temperatures, facilitating the mobility of carbon atoms that can form the graphene domains leading to lower lattice defects. For this reason, the Cu surface morphology at high growth temperature is a key parameter that determines the morphological aspects of graphene film. In the surface mechanism of graphene growth on Cu, it is known that graphene fragments grow when the growth temperature is completely enough to accelerate the diffusion of fragments and thus, some fragments may coalesce to form a larger domain [65].

2.4.1(b) Pre-treatment of Copper

Cu foils are usually treated before graphene growth. These treatments ensure high-quality graphene deposition consisting of relatively large domain sizes. It is known that the native copper oxide (CuO_2, CuO) that covers the received Cu foil usually decreases its catalytic impact. Thus, the copper substrate undergoes annealing process in the hydrogen (H_2) atmosphere at 1000°C to reduce the copper oxides to the minimum limit. Meanwhile, dipping the copper foils in acetic acid as a wet chemical treatment